Theor Chem Acc (2005) 114: 200–207
DOI 10.1007/s00214-005-0661-0

REGULAR ARTICLE

P.K. Nandi · K. Mandal · T. Kar

# Ab initio SCRF study of solvent effect on the nonlinear polarizabilities of different intramolecular charge-transfer molecules

Received: 10 August 2004 / Accepted: 4 December 2004 / Published online: 14 July 2005


**Abstract** The macroscopic solvent effect on static nonlinear polarizabilities of a number of intramolecular charge-transfer (ICT) molecules have been studied by using the self-consistent-reaction field (SCRF) model in the framework of ab initio time-dependent-HF (TDHF) method using 3-21G basis set. The two-state model of static $\beta$ and $<\gamma>$ have been used to obtain their functional dependence on the ground-state hardness parameter, dipole moment and solvation energy. The methyl substituted 4-quinopyran and other zwitterionic molecules are found to exhibit strong diminution of both quadratic and cubic polarizabilities at higher solvent reaction field due to negative solvatochromic effect. However, molecules showing positive solvatochromism lead to strong enhancement of the NLO response on increase in solvent polarity. The evolution pattern of the solvent modulated static $\beta$ and $<\gamma>$ of 4-quinopyran (4QP) obtained for varying inter-ring torsion angle differ strikingly from that shown by $p$-amino $p'$-nitro biphenyl (ANB).

**Keywords** Static first- and second-hyperpolarizabilities ($\beta$ and $<\gamma>$) · 2-state model · Hardness parameter ($\eta$) · SCRF model

## 1 Introduction

Nonlinear optics (NLO) is an active area of current research. Substances able to manipulate photonic signals efficiently are of importance in opto-electronics. Amongst these, the molecule-based macroscopic $\pi$-electron assemblies have been found to possess many attractive NLO characteristics. Moreover, the NLO response of these materials originates from the NLO characteristics of the constituent molecules. Quite a large number of experimental [1–7] and theoretical studies [8–20] showed that the NLO properties of charge-transfer (CT) chromophores can be strongly modulated due to its interaction with the environment. The influence of solvent on the second- and third-order polarizabilities has usually been studied by using different continuum solvent models in the framework of semiempirical and ab initio quantum mechanical methods. Amongst the continuum solvent models the self-consistent reaction-field (SCRF) model [21–23] and its extended versions [24,25] have been widely used [10–14] in the study of the solvatochromic properties, and the linear and nonlinear optical properties of many CT chromophores with a fair degree of success. Recently, the polarizable continuum model (PCM) in the framework of CPHF and time-dependent-HF (TDHF) methods have been used [26] to estimate the dispersion and repulsion contributions to the NLO properties of molecules in solutions. However, only very few attempts [18,27] have been made to study the NLO property of small push–pull polyenes within PCM.

The earlier theoretical study [28] of the first-hyperpolarizability of 4-quinopyran (4QP) in the gas phase predicted rather strong enhancement of static $\beta$ upon twisting the rings. The methyl substituted 4QP having a twisted ring structure showed higher $\beta$ values. The enhancement of $\beta$ occurs as a result of increased CT interaction in the transition from neutral quinoid to charged benzenoid structure. The presence of solvent is thus expected to strongly modulate the CT interaction and the NLO properties of 4QP. Moreover, the quinoid molecules are known [29] to be highly sensitive to the external electric field to modulate electric response properties. However, there remains considerable lack of information regarding the influence of solvent on the NLO properties of quinoid type of molecules. We, therefore, intend to undertake a theoretical study of the solvent effect on the static second- ($\beta$) and third-order ($\gamma$) polarizabilities of 4QP (1a–d) and other related twisted intramolecular charge-transfer (TICT) molecules (2a–f, in Scheme 1) in a semiquantitative manner. The prototype molecules, $p$-nitro aniline (PNA)

P.K. Nandi (✉) · K. Mandal
Department of Chemistry,
Bengal Engineering and Science University,
Shibpur, Howrah 711 103, India.
Fax: +91-033-26682916,
E-mail: nandi_pk@yahoo.co.in, tapaskar@cc.usu.edu

T. Kar
Department of Chemistry and Biochemistry,
Utah State University, Logan, UT, 84322 – 0300, USA

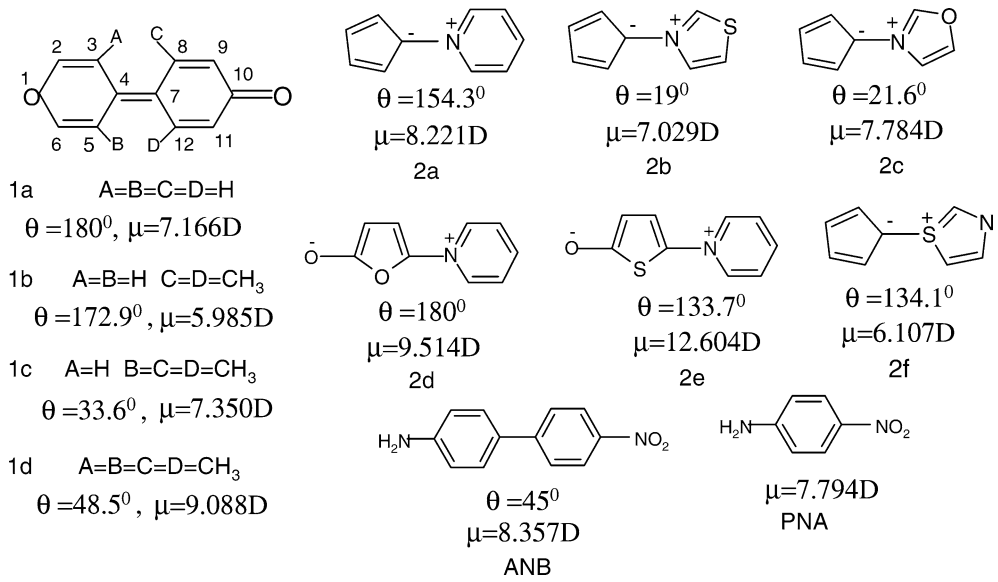


**Scheme 1** (Selected molecules along with the gas-phase optimized inter-ring torsion angle ($\theta$) and the dipole moment ($\mu$))

and ANB have also been included for the sake of comparison. The macroscopic solvent effect on the NLO properties has been calculated by using the SCRF model in the framework of ab initio MO method. Since the chosen molecules possess significant ground-state dipole moment and are not polyene-like, the consideration of spherical cavity and the dipolar interaction within the SCRF model is expected to provide meaningful results. The solvents used for the present study include cyclohexane ($\varepsilon = 2.0$), chloroform ($\varepsilon = 4.8$), THF ($\varepsilon = 7.6$), dichloromethane ($\varepsilon = 9.1$), acetone ($\varepsilon = 20.7$), acetonitrile ($\varepsilon = 36.6$), DMSO ($\varepsilon = 46.7$) and water ($\varepsilon = 78.4$). The two-state expressions of the NLO parameters have been used to find any correlation with the ground-state dipole moment, hardness parameter and solvation energy in solvents with varying degree of polarity.

## 2 Method of calculations

The ground-state geometry of the chosen molecules have been fully optimized at the RHF/3-21G level in the gas phase and in solution. Excepting for 1a and 2d (Scheme 1), the majority of the molecules have nonplanar equilibrium geometry. In the case of 4QP and ANB the geometry of each conformer has been optimized for different values of inter-ring torsion angle ($\theta$). The RHF/3-21G optimized geometry of the molecules has been used in the single point TDHF/3-21G calculation of the static quadratic and cubic polarizabilities. All calculations have been performed with GAMESS programs [30] using the options ICUT=20, ITOL=30 and INTTYP=HONDO to achieve greater accuracy in the calculated NLO parameters.

The static $\beta_{\text{vec}}$ has been calculated by using the following expressions [31].

$$\beta_{\text{vec}} = \sqrt{(\beta_x^2 + \beta_y^2 + \beta_z^2)}, \tag{1}$$

where $\beta_i (i = x, y, z)$ is given by,

$$\beta_i = (1/3) \sum_{j=x,y,z} (\beta_{ijj} + \beta_{jij} + \beta_{jji})$$

The static average cubic polarizability, $\langle\gamma\rangle$ has been calculated by using the following relation [32],

$$\langle\gamma\rangle = \left(\frac{1}{5}\right)[\gamma_{xxxx} + \gamma_{yyyy} + \gamma_{zzzz} + 2(\gamma_{xxyy} + \gamma_{xxzz} + \gamma_{yyzz})]. \tag{2}$$

The above expressions show that $\beta_{\text{vec}}$ must be always positive while the $\langle\gamma\rangle$ may have positive or negative sign. In the two-state model, the static linear ($\alpha$), first-hyperpolarizability ($\beta$) and second-hyperpolarizability ($\gamma$) can be written [33] as follows:

$$\alpha = \frac{2(\mu_{ge})^2}{\Delta E}, \tag{3}$$

$$\beta = \left(\frac{3}{2}\right)\Delta\mu\frac{f_0}{\Delta E^3}, \tag{4}$$

$$\gamma = \frac{\mu_{ge}^2\Delta\mu^2}{\Delta E^3} - \frac{\mu_{ge}^4}{\Delta E^3} = \frac{(\Delta\mu^2 - \mu_{ge}^2)3f_0}{2\Delta E^4}, \tag{5}$$

where $\Delta E$ is the transition energy between the ground ($\langle g|$) and the lowest lying excited ICT state ($\langle e|$), $f_0$ (=$(2/3)\Delta E\mu_{ge}^2$) is the oscillator strength and $\Delta\mu (= e_0\{\langle e|r|e\rangle - \langle g|r|g\rangle\}$, $e_0$= charge on electron) is the difference between the ground- and excited-state dipole moment and $\mu_{ge} (= e_0\langle g|r|e\rangle)$ is the electronic transition moment integral. The calculated dipole moment is expressed in Debye and polarizabilities are presented in esu units as $\alpha$ (in $10^{-23}$), $\beta$ (in $10^{-30}$) and $\gamma$ (in $10^{-36}$).

The solvent-modified NLO parameters have been calculated by using the SCRF model in the framework of TDHF method in which solvent-modified fully optimized geometry of the molecules are used. In GAMESS, the version A of the SCRF model [25] based on the classical Kirkwood–Onsager theory [21,22] has been implemented. In the reaction-field (RF) approach, the solute molecule with a permanent dipole moment ($\mu$) is placed in a spherical cavity of radius ($r$) in a dielectric continuum with static dielectric constant $\varepsilon$. The electric-field of the solute will polarize the surrounding media and the induced-field also called the reaction-field ($R$) will act on the solute.

$$R = g\mu, \tag{6}$$

where $g$, is Onsager constant which is given by $g = (2/r^3)$ $f(\varepsilon)$. In Eq. (6) $\mu$ corresponds to the dipole moment of solute in the gas phase. If the solvent is assumed to be fully equilibrated then $f(\varepsilon) = (\varepsilon - 1)/(2\varepsilon + 1)$. However, in this approximation, the solvent RF will be almost insensitive to change in solvent polarity at higher dielectric region where $f(\varepsilon)$ tends to be a constant (0.5). In the MO theory the solute–solvent interaction is taken into account by incorporating a perturbation term $V$ in the Hamiltonian ($H_0$) of the isolated solute molecule, that is, $H = (H_0 + V)$ where

$$\begin{aligned} V &= -\left(\frac{1}{2}\right)\mu \cdot R \\ &= -\left(\frac{1}{r^3}\right) f(\varepsilon)\mu\langle\psi|\mu|\psi\rangle \\ &= -kf(\varepsilon)\mu\mu_g. \end{aligned} \tag{7}$$

Using this interaction Hamiltonian the pertinent Schrodinger equation can be solved in the framework of the time-dependent Hartree–Fock theory to obtain the solvent modified MOs and energies. The total energy of solute in the presence of the RF is then given by

$$E = E_0 - 1/2g\mu_g^2. \tag{8}$$

In Eq. (8) $E_0$ is the gas-phase energy of the solute and the second term represents the electrostatic energy of solvation in the ground state. $\mu_g$ represents the corresponding solvent-corrected dipole moment of solute.

Regarding the choice of cavity radius (r) there are two conventions generally found in the literature. In one case $r$ is taken as half the distance between the leftmost and rightmost atoms of the molecule plus the van der Waals radii of the two atoms. Alternatively $r$ can also be estimated from the molar mass ($M$) and density ($d$) of the solute as follows:

$$r = 0.7346\left(\frac{M}{d}\right)^{1/3}. \tag{9}$$

It has been found [13] that the value of r obtained by using Eq. (9) is about 60–70% of the cavity radius including van der Waals radii. For a given solvent the RF corresponding to larger $r$ is found to be about 24% of that associated with smaller $r$. In the present study two different values of $r$ have been used for each molecule in SCRF calculations. The RF associated with the smaller and higher values of $r$ will be referred to as higher (HRF) and lower (LRF) reaction fields, respectively. The cavity radius used in HRF calculation is taken as half the distance between the leftmost and rightmost atoms of the solute. This radius has been found to lie within 60–64% of that used in LRF.

For the single excitation, HOMO ($\phi_i$) $\rightarrow$ LUMO ($\phi_j$) in the closed-shell single determinant, the corresponding vertical transition energy ($\Delta E$) is given by

$$\Delta E = \varepsilon_j - \varepsilon_i + (2K_{ij} - J_{ij}) = 2\eta + A, \tag{10}$$

where $\eta$ refers to the molecular hardness parameter which is equal to half of the HOMO–LUMO energy difference [34], and the constant $A$ corresponds to the difference of the exchange and repulsion integrals which is usually negative and quite large. In our recent studies [35,36] it has been shown that the two-state model of $\beta$ (Eq. (4)) using $\eta$ in place of $\Delta E$ can satisfactorily correlate with static $\beta_{\text{vec}}$ in donor–acceptor substituted heterocycles and sesquifulvalene molecules. The hardness parameter has been found to follow linear correlation with the bond length alteration (BLA) parameter. The smaller BLA and $\eta$ correspond to stronger CT interaction.

The solvent modified energy of the ground ($E_g$) and excited state ($E_e$) of the solute, assuming the complete equilibration of solvent can be written as

$$E_g = E_g^0 - \frac{1}{2}\left(\frac{2}{r^3}\right) f(\varepsilon)\mu_g^2 \tag{11}$$

$$E_e = E_e^0 - \frac{1}{2}\left(\frac{2}{r^3}\right) f(\varepsilon)\mu_e^2 \tag{12}$$

The transition energy ($\Delta E$) estimated by subtracting Eq. (11) from Eq. (12) corresponds to the vertical excitation energy which in conjunction with the approximation, $\mu_e = a\mu_{\text{g}}$ (a being a positive factor) can be expressed as

$$\begin{aligned} \Delta E(\varepsilon) &= \Delta E^0 - \frac{1}{2}\left(\frac{2}{r^3}\right) f(\varepsilon)\mu_g^2(a^2 - 1) \\ &= \Delta E^0 + E_s^g(a^2 - 1), \end{aligned} \tag{13}$$

where $\Delta E^0 (= \Delta E(\varepsilon = 1))$ is the gas-phase transition energy and $E_s^{\text{g}} = -1/2(2/r^3) f(\varepsilon)\mu_g^2$ is the ground-state solvation energy of solute. For a given molecule the factor a can be taken as nearly constant in different polar solvents, and can be expressed as the ratio of the dipole moment and square root of solvation energy of the two states as follows:

$$a^2 = \frac{\mu_e^2}{\mu_g^2} = \frac{E_s^e}{E_s^g} \tag{14}$$

Two distinct kinds of solvent effects on $\Delta E$ ($\varepsilon$) can be anticipated, red-shifting for $a > 1$ and blue-shifting for $a < 1$.

The functional dependence of $\beta$ on $\eta$ can be derived using the static two-state model expression of $\beta$ (Eq. (4)). While deriving it has been assumed that the oscillator strength ($f_0$) of the molecule can be regarded as a constant, independent of the variation of solvent RF or charge polarization due to conformation changes or varying electron push–pull groups. This can be justified if $\Delta E$ or $\eta$ and $1/\alpha^{1/2}$ bear a linear relationship which can be shown to exist as follows.

By making use of the expression of oscillator strength, $f_0 = (2/3)(\mu_{ge})^2 \Delta E$ and the two-state form of $\alpha = 2(\mu_{ge})^2/\Delta E$ (Eq. (3)), the following relation between $\alpha$ and $f_0$ can be obtained,

$f_0 = \alpha \Delta E^2/3$ which using Eq. (10) can be written as

$$\eta = c f_0^{1/2}(1/\alpha^{1/2}) - A \tag{15}$$

where c is a constant. In fact, we obtained a linear correlation between $\eta$ and $1/\alpha^{1/2}$ for different types of push–pull molecules in the gas phase, and here for the chosen molecules in different polar solvent. Now the quadratic polarizability in Eq. (4) can be correlated to the ground-state CT parameters as

$$\beta \propto (a-1)\mu_g/(2\eta)^3 \tag{16}$$

The calculated $\beta$ is expected to bear a linear relationship with $\mu_g/(2\eta)^3$ provided the factor a remains insensitive to the ground-state polarization. The slope of $\beta$ versus $\mu_g/(2\eta)^3$ plot for solvents with increase in $\varepsilon$ should be positive for $a > 1$ and negative for $a < 1$ which correspond to the positive and negative solvatochromic effects, respectively on solute's CT transition.

Let us now find the functional dependence of $\beta$ and $\langle\gamma\rangle$ on the ground-state solvation energy ($E_s^g$)of the solute. Eq. (16) can also be written as

$$\beta = k\mu_g/(\Delta E)^3$$

$$\begin{aligned}\beta/\mu_g &= k/(\Delta E)^3 \\ &= k[\Delta E^0 + E_s^g(a^2-1)]^{-3}(\text{using Eq. (13)}) \\ &= k/(\Delta E^0)^3[1 + E_s^g(a^2-1)/\Delta E^0]^{-3}\end{aligned}$$

Expanding the second factor up to the cubic term and rearranging one gets,

$$\begin{aligned}\beta/\mu_g = {} & k/(\Delta E^0)^3 - \{3k(a^2-1)/(\Delta E^0)^4\}(E_s^g) \\ & +\{6k(a^2-1)^2/(\Delta E^0)^5\}(E_s^g)^2 \\ & -\{10k(a^2-1)^3/(\Delta E^0)^6\}(E_s^g)^3\end{aligned} \tag{17}$$

Neglecting all terms beyond the second, the slope of the $\beta/\mu_g$ versus ($-E_s^g$) plot should be positive for $a > 1$ and negative for $a < 1$.

Using the expressions of $f_0$ and the two-state expression of $\alpha$, the dipolar (D) and the negative ($N$) terms in Eq. (5) can be expressed as

$$\begin{aligned}\gamma &= 3\Delta\mu^2 f_0/2\Delta E^4 - 3\alpha f_0/4\Delta E^3 \\ \gamma &= 3(a-1)^2\mu_g^2 f_0/2\Delta E^4 - 3c\mu_g^2 f_0/4\Delta E^3 \\ \gamma/\mu_g^2 &= k_1/\Delta E^4 - k_2/\Delta E^3\end{aligned} \tag{18}$$

where $k_1 = 3(a-1)^2 f_0/2$ and $k_2 = 3cf_0/4$. The constant $c$ is taken as the proportionality constant between the solvent modified $\alpha$ and $\mu_g^2$. This correlation has been found to exist for the chosen molecules, and is thereby used to simplify the two-state expression of $\gamma$. Considering the vertical transition approximation for $\Delta E$ (Eq. (13)) and on expanding $\Delta E^{-n}$ Eq. (18) can be transformed into the following form.

$$\begin{aligned}\gamma/\mu_g^2 = {} & \{k_1/(\Delta E^0)^4 - k_2/(\Delta E^0)^3\} + \{3k_2(a^2-1)/(\Delta E^0)^4 \\ & -4k_1(a^2-1)/(\Delta E^0)^5\}E_s^g \\ & +\{10k_1(a^2-1)^2/(\Delta E^0)^6 \\ & -6K_2(a^2-1)^2/(\Delta E^0)^5\}(E_s^g)^2 + \cdots \\ \gamma/\mu_g^2 = {} & (d_0 - n_0) - (d_1 - n_1)E_s^g \\ & +(d_2 - n_2)(E_s^g)^2 + \cdots\end{aligned} \tag{19}$$

The constants $d_i$ and $n_i$ correspond to the coefficients in the polynomial expansion of $D$ and $N$ terms in $E_s^g$. It is to be noted that excepting $d_1$ and $n_1$ the remaining coefficients are always positive. $d_1$ and $n_1$ are both positive (negative) for $a > 1 (a < 1)$. The sign of $\gamma$ depends on the these coefficients. Considering only the linear term it can be seen that for a dominant contribution of the dipolar term, the slope in the $\gamma/\mu_g^2$ versus $(-E_s^g)$ plot should be positive for $a > 1$ and negative for $a < 1$. However, the pattern will be reversed if the negative term contributes dominantly.

## 3 Results and discussions

In order to assess the performance of the SCRF model and the choice of the basis set in the calculation of the solvent modified NLO parameters we have plotted (Fig. 1a) the calculated static $\beta_{vec}$ of PNA against the experimentally available static $\beta$ estimated from HRS [14] and EFISH [1] measurements in different polar solvents. Our calculated $\beta$ values show a fairly good agreement ($R = 0.92$ and SD = 0.3−0.4) with both sets of $\beta_{exp}$. Since experimental static $\beta_{exp}$ are estimated from the two-state expression of $\beta$, the linear plots in Fig. 1a implies that the lowest excited CT state provides a major contribution to the quadratic polarizability. The 6-31G* calculated $\beta$ values are found to be smaller compared to the 3-21G and 6-31+G* values. In order to find correlation between $\eta$ and $\Delta E$, we have plotted (Fig. 1b) our calculated solvent-modified $\eta$ values against $\Delta E$ corresponding to the available CT absorption maximum of PNA [1] in different polar solvents. A good linear relationship ($R = 0.95$ and SD = 0.004) between $\eta$ and $\Delta E$ holds for both 3-21G and 6-31+G* basis sets. Thus molecular hardness parameter can be useful for qualitatively accounting for the solvent modulation of CT transition energy (see Eq. (10)). Based on the above-mentioned correlations between the calculated and experimental results, it seems that the SCRF method and the 3-21G basis set used in the TDHF calculations of NLO parameters would be able to predict qualitative trends fairly reliably.

Our calculated gas-phase static $\beta$ (28.8) of ANB agrees fairly with that (21.7) obtained by others [19]. The variation of static $\beta$ of ANB with increasing solvent polarity is shown in Fig. 2a. The linear plots in Fig. 2a are in good agreement with Eqs. (16) and (17), and also consistent with earlier work reported for ANB [19,37]. An exactly similar linear correlation is also found to exist between $\gamma/\mu_g^2$ and $(-E_s^g)$ (Fig. 2d).

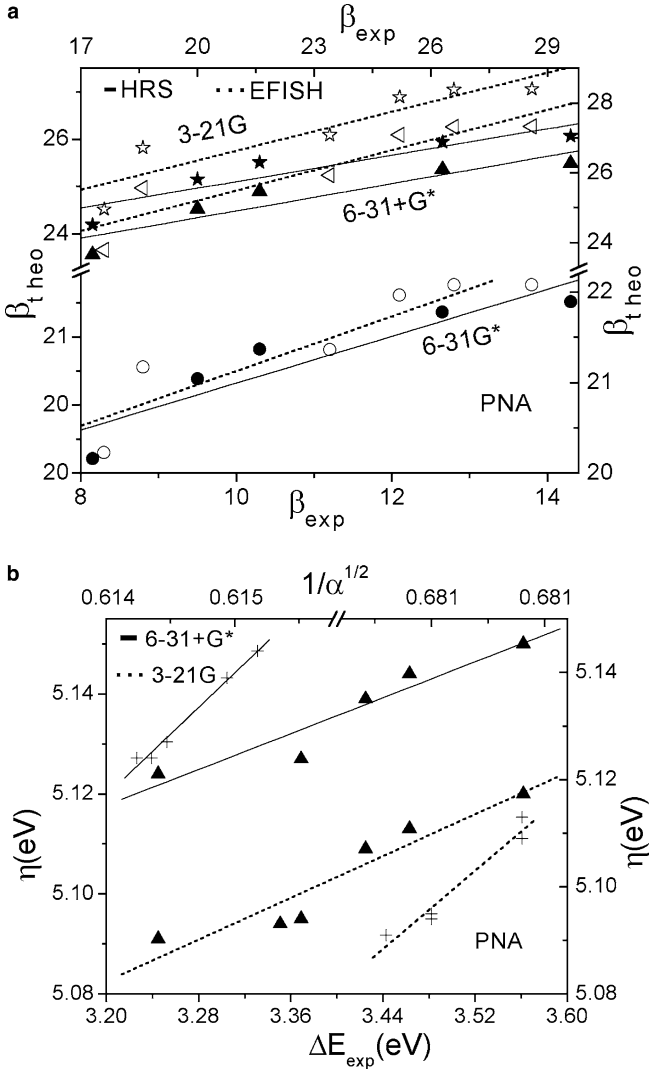


**Fig. 1** Plot of calculated **a** static $\beta$ obtained at 3-21G (*star*), 6-31G* (*circle*) and 6-31+G* (*triangle*) against the experimental static $\beta$ estimated from EFISH [1] and HRS [14] measurements in $\varepsilon$ = 2.2, 4.8, 6.02, 7.25, 20.7, 36.71 and 37.5 for PNA **b** $\eta$ versus experimental $\Delta E$ (▲) and $\eta$ versus $1/\alpha^{1/2}$ (+) of PNA [1] in $\varepsilon$ = 4.8, 6.02, 7.58, 20.7, 32.63 and 36.71. In all figures (excepting Fig.4) the combination of axes refer to (1) left versus bottom and (2) right versus top

### 3.1 The solvent modulation of NLO properties of 4QP

The influence of solvent on the first-hyperpolarizability of 4QP is shown in Fig. 2b and c, respectively. The static $\beta$ (12.74 in gas phase) is found to be strongly modulated in polar solvents, especially for HRF. The calculated static $\beta$ obtained for LRF and HRF are found to increase with increase (decrease) in dipole moment (hardness parameter), which is consistent with Eq. (16). This pattern of variation of $\beta$ is exactly similar to that obtained for ANB (Fig. 2a). The linear relationship between $\eta$ and $\alpha^{1/2}$ at different RFs indicates that oscillator strength remains insensitive to changes in solvent polarity. The functional dependence of $\beta$ on the ground-state solvation energy ($E_s^g$) is found (Fig. 2c) to be different for lower and higher RFs. At LRF the pattern of variation is linear and is identical to that shown by ANB. However, at HRF, $\beta$ varies cubically with $E_s^g$ (3-21G: $R^2 = 0.99998$, SD = 0.005) and is consistent with Eq. (17). It can be seen that the pattern of variation does not depend on the basis set. Thus a quinoid molecule at lower RF can exhibit close similarity with a benzenoid molecule in the matter of variation of static $\beta$.

The response pattern of second-hyperpolarizability of 4QP in polar solvents is shown in Fig. 2d. The calculated $\langle\gamma\rangle/\mu_g^2$ is found to increase linearly with $(-E_s^g)$. This remarkably good linear correlation occurs both at LRF and HRF cases. The substituted 4QP, 1d at lower RF exhibit (not shown) similar trend as obtained for ANB. It is important to note that the calculated static $\alpha$ for these molecules has been found to vary quadratically with $\mu_g$. These results are in fair agreement with that predicted by Eq. (19).

### 3.2 The influence of solvent on NLO parameters in TICT molecules

The calculated static $\beta$ ($\eta$) of 2a–f in the gas phase/solvent ($\varepsilon$ = 46.7 at HRF) are 154.08 (3.755)/39.0 (4.425), 96.71 (3.891)/32.29 (4.563), 57.28 (4.275)/17.19 (4.958), 129.75 (3.456)/86.92 (4.121), 45.51 (3.641)/17.02 (4.235) and 28.18 (4.137)/16.83 (4.528), respectively. The experimental and other theoretical (SCRF in INDO/S at HRF) studies of solvent effect of 2a also showed [8] a large blue-shifting in the $\pi$–$\pi^*$ transition. The solvent dependence of static $\beta$ and $\gamma$ of molecules 2a–f is shown in Fig. 3a–c. It can be seen that static $\beta$ decreases with increase in solvent polarity, but the effect is more pronounced for higher RF. The lowering of $\beta$ with increase in dielectric constant occurs primarily due to the increase in $\Delta E$ since $\beta$ (Eq. (4)) is more sensitive to $\Delta$E rather than $\mu_g$. Since the molecules, 2a–f are highly polar in the ground state, the increasingly higher solvation energy in solvent with large $\varepsilon$ causes significant blue-shift in $\Delta E$ (increase in $\eta$) which in turn leads to rather significant lowering in $\beta$. This has been reflected in the $\beta/\mu_g$ versus $E_s^g$ plots in Fig. 3b which is also in conformity with Eq. (17). The calculated static $\langle\gamma\rangle$ also follows a sharp decreasing trend with increase in $\varepsilon$. The $\gamma/\mu_g^2$ versus $(-E_s^g)$ plots (Fig. 3c) for the zwitterionic molecules are found to be linear which is consistent with Eq. (19).

Although not shown here, the similar linear plots (Fig. 3b–c) have been found for the methyl substituted 4QP (1b–d) for higher RF. In contrast the pattern at LRF follows an increasing trend rather similar to that of 4QP (Fig. 2c). With increasing methyl substitution at the inter-ring sites the ground-state of 4QP has been found to be increasingly polar which at higher RF leads to rather strong diminution of both $\beta$ and $\langle\gamma\rangle$. It should be mentioned that the inter-ring torsion angle in methyl substituted 4QPs gradually shifts toward 90° with increase in $\varepsilon$ at HRF. The corresponding NLO parameters are found to attain the lowest value at 90°. The solvent effect on 1a and 1d shows an opposing trend. The calculated static $\beta$

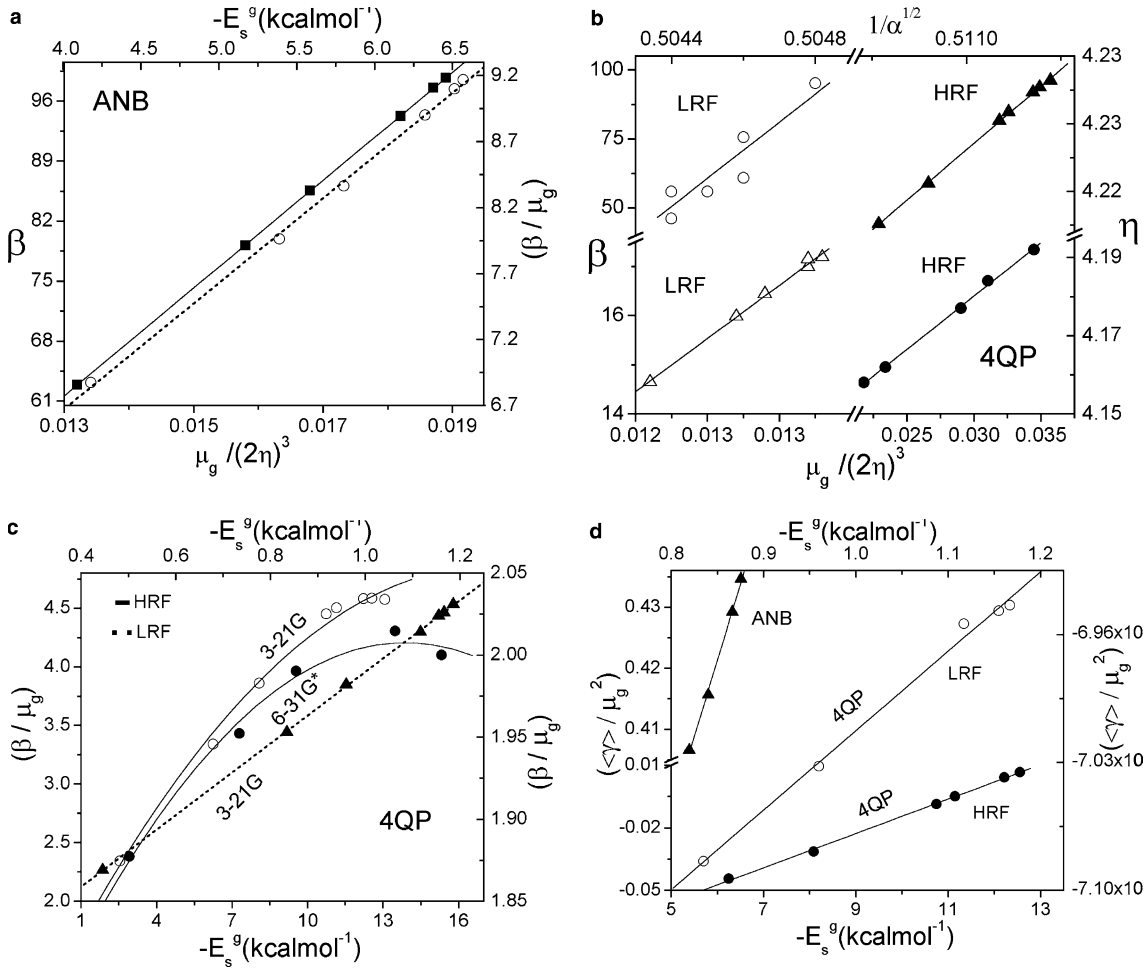


**Fig. 2** Plot of calculated **a** static $\beta$ versus $\mu_g/(2\eta)^3$ (■) and $\beta/\mu_g$ versus ground-state solvation energy $(-E_s^g)$ (o), respectively for ANB, **b** $\beta$ versus $\mu_g/(2\eta)^3$ (*triangle*) and $\eta$ versus $1/\alpha^{1/2}$ (*circle*), respectively for 4QP at different RFs, **c** $\beta/\mu_g$ versus $(-E_s^g)$ for 4QP at 3-21G and 6-31G* basis sets, respectively, **d** $\langle\gamma\rangle/\mu_g^2$ versus $(-E_s^g)$ for ANB (*triangle*) and 4QP (*circle*)

of 1a and 1d in gas phase/water (at HRF) are 12.74/96.19 and 62.54/10.28, respectively.

### 3.3 The difference in the NLO response patterns shown by quinoid and nonquinoid type chromophores

The evolution pattern of the static linear and nonlinear polarizabilities of 4QP calculated for different inter-ring torsion angles ($\theta$) (0 – 90°) in a solvent with $\varepsilon = 46.7$ at LRF and HRF are shown in Fig. 4a–b. The corresponding evolution pattern of ANB at a higher RF is also presented in Fig. 4c for the sake of comparison. It should be mentioned that the calculated RF is found to increase with $\theta$ for 4QP while it decreases for ANB. Although not shown it has been found that the evolution pattern of NLO parameters of 4QP at LRF (Fig. 4a) is almost identical to that obtained for variation in the NLO response of solvent free 4QP as a function of $\theta$. It would be worth mentioning that in the lower field case calculated $\eta$ (not shown in the Figure) has been found to exhibit a gradually decreasing trend with RF which accounts for the increasing trend in $\alpha$ and $\beta$ (Fig. 4a) as expected from their two-state expressions (Eqs. (3) and (4)). The increasingly negative $\gamma$ can similarly be ascribed to the lowering in $\Delta E$ and increase in $\alpha$ in the dominant N term (Eq. (18)).

At HRF static $\beta$ and $\gamma$ have been found to exhibit (Fig. 4b) maxima at $\theta = 40°$ and 60°, respectively. The calculated $\alpha$ shows a monotonically decreasing trend while $\mu_g$ shows an increasing trend with $\theta$. The appearance of maximum in $\beta$ and $\gamma$ can be explained by using the two-state model. The increasing trend of $\beta$ may be ascribed to the dominant contribution of $\mu_g$ while the lowering in $\beta$ is expected to occur due to the blue-shifting in $\Delta E$ (Eq. (16)). Before the occurrence of maximum of $\gamma$, the dipolar term (D) predominates over the negative term (N) due to sharp rise in $\mu_g$ and lowering in $\alpha$ (see Eq. (18)). But beyond the maximum the contribution of D is decreased due to the smaller change in $\mu_g$.

In the ground state of ANB the inter-ring angle ($\theta$) has been found to be 45° in the gas phase and 41.2° in DMSO. The evolution pattern of ANB (Fig. 4c) shows qualitatively a

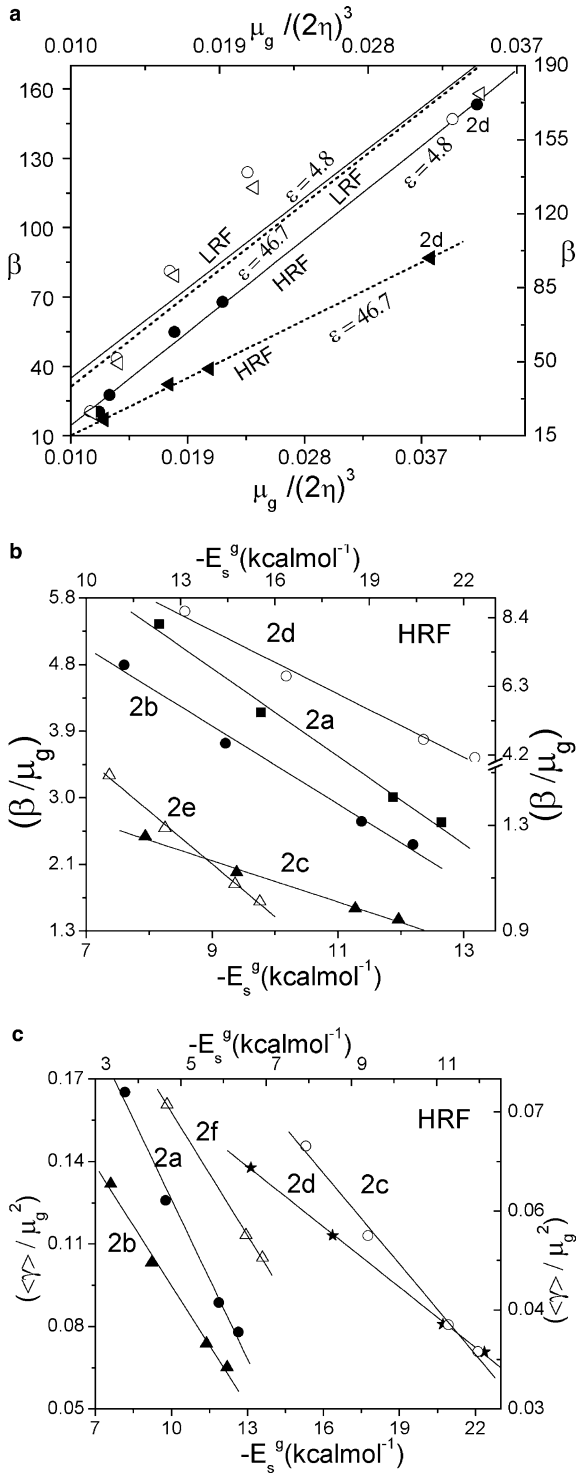


**Fig. 3** Plot of calculated **a** static $\beta$ against $\mu_g/(2\eta)^3$ for molecules 2a–2f (Scheme 1) for $\varepsilon = 4.8$ (*solid line*) and 46.7 (*dotted line*) for LRF and HRF, respectively, **b** static $\beta/\mu_g$ versus $(-E_s^g)$ for molecules 2a–2e and (c) $\langle\gamma\rangle/\mu_g^2$ versus $(-E_s^g)$ for molecules 2a–2d and 2f, for $\varepsilon = 4.8$, 7.6, 20.7 and 46.7 at HRF

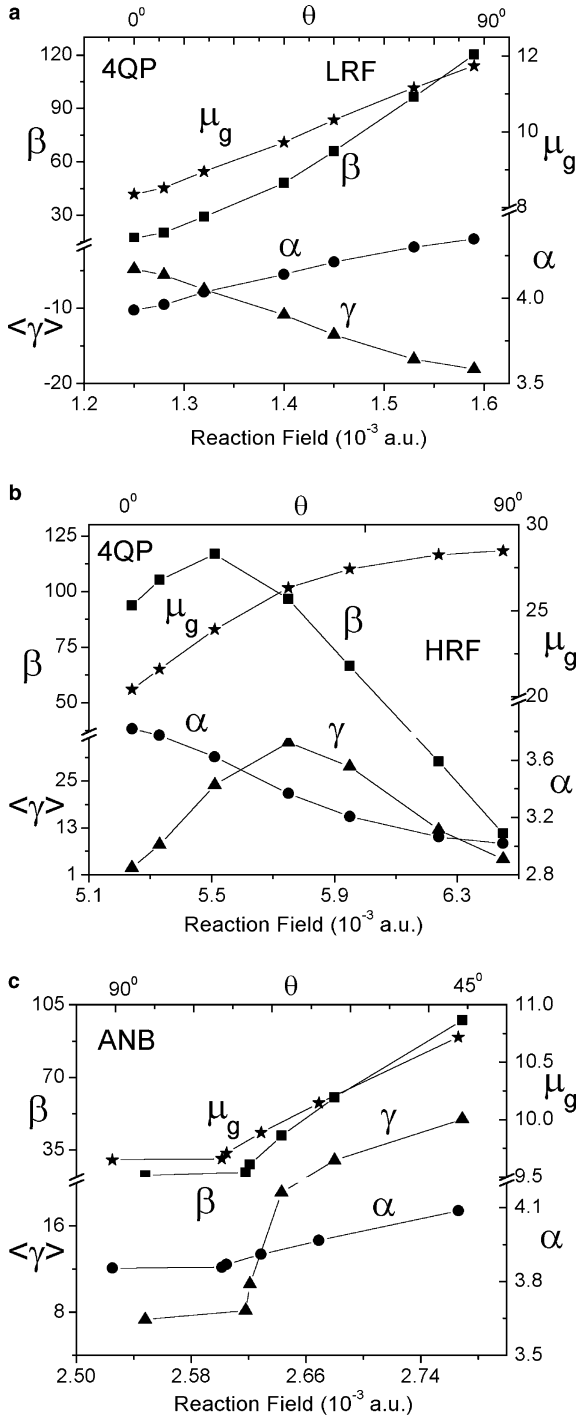


**Fig. 4** Evolution pattern of the ground-state dipole moment and static polarizabilities as a function of calculated solvent RF (for $\varepsilon = 46.7$) obtained for each inter-ring twist angle ($\theta$) for 4QP ($\theta = 0 - 90^\circ$) at **a** LRF and **b** HRF, and **c** ANB ($\theta = 45 - 90^\circ$) at HRF

parallel trend when compared to that of 4QP at LRF (Fig. 4a). However, an exactly opposing trend is found for variation with respect to $\theta$. Again the decreasing trend of the polarizabilities with $\theta$ (Fig. 4c) can be explained by the two-state model for increase in $\Delta E$. Indeed, our calculated $\eta$ has been found to increase with increase in $\theta$ or decrease in RF for ANB molecule.

## 4 Conclusion

The present study considers a number of CT molecules, the ground-state dipole moments of which are comparable to that of the prototype PNA and ANB molecules. The quadratic and cubic polarizabilities of the chosen species have been calculated in the gas phase and in solvents having varying degree of polarity. The response pattern of the static NLO parameters have been rationalized by considering the two-state model. It can be seen that the solvent-modified $\beta$ and $\gamma$ of quinoid molecules (1a–d) reveal remarkably different trends compared to what is shown by molecules (2a–f) in Scheme 1. The former species at the LRF, are found to exhibit rather close similarity with the bezenoid chromophore, ANB in the variation of NLO properties which generally increase with increase in $\varepsilon$. The enhancement of $\beta$ and $\gamma$ in these molecules primarily arises from the red-shift in $\Delta E$ (decrease in $\eta$). In contrast, molecules, 2a–f exhibit a reverse trend in the pattern of variations of solvent-modified NLO parameters which in the present study are found to decrease appreciably. This may be ascribed to the rather strong negative solvatochromic effect as indicated by larger $\eta$ and $\mu_g$ values in solvents with higher polarity. Finally, the evolution of NLO parameters of 4QP with varying inter-ring torsion angle in DMSO has been compared to that of ANB. Although the evolution pattern of $\beta$ and $\gamma$ of 4QP significantly differ for LRF and HRF, the corresponding evolution pattern of ANB is found to be rather independent of the RF.

**Acknowledgements** KM is thankful to CSIR, Government of India, New Delhi, for providing her with Senior Research Fellowship.

## References

1. Stahelin M, Burland DM, Rice JE (1992) Chem Phys Lett 191:245–250
2. Clays K, Hendrickx E, Triest M, Verbiest T, Persoons A, Dehu C, Bredas JL (1993) Science 262:1419
3. Marder SR, Gorman CB, Meyers F, Perry JW, Bourhill G, Bredas JL, Pierce BM (1994) Science 265:632
4. Bourhill G, Bredas JL, Cheng L-T, Marder SR, Meyers F, Perry JW, Tiemann BG (1994) J Am Chem Soc 116:2619
5. Runser C, Fort A, Barzoukas M, Combellas C, Suba C, Thiebalt A, Graff R, Kintzinger JP (1995) Chem Phys 193:309
6. Woodford JN, Pauley MA, Wang CH (1997) J Phys Chem A 101:1989
7. Huyskens FL, Huyskens PL, Persoons PA (1998) J Chem Phys 108:8161
8. Karelson MM, Zerner MC (1992) J Phys Chem 96:6949
9. Sen R, Majumdar D, Bhattacharyya SP (1992) Chem Phys Lett 190:443–446
10. Willets A, Rice JE (1993) J Chem Phys 99:426
11. Yu J, Zerner MC (1994) J Chem Phys 100:7487
12. Bella SD, Marks TJ, Ratner MA (1994) J Am Chem Soc 116:4440–4445
13. Albert IDL, Marks TJ, Ratner MA (1996) J Phys Chem 100:9714–9725, and references therein
14. Dehu C, Meyers F, Hendrickx E, Clays K, Persoons A, Marder SR, Bredas JL (1995) J Am Chem Soc 117:10127–10128, and references therein
15. Allin SB, Leslie TM, Lumpkin RS (1996) Chem Mater 8:428–432
16. Larsson P-E, Kristensen ML, Mikkelsen KV (1999) Int J Quantum Chem 75:449
17. Luo Y, Norman P, Macak P, Ågren H (1999) J Chem Phys 111:9853 and references therein
18. Luo Y, Norman P, Macak P, Ågren H (2000) J Phys Chem A 104:4718
19. Lipinski J, Bartkowiak W (2001) J Phys Chem A 105:10702–10710, and references therein
20. Laage D, Thompson WH, Blanchard-Desce M, Hynes JT (2003) J Phys Chem A 107:6032–6046
21. Onsager L (1936) J Am Chem Soc 58:1486
22. Kirkwood JG (1939) J Chem Phys 7:911
23. Tapia O, Goscinski O (1975) Mol Phys 29:1653
24. Rivail J, Rinaldi D (1976) Chem Phys 18:223
25. Szafran M, Karelson MM, Katritzky AR, Koput J, Zerner MC (1993) J Comput Chem 14:371–377
26. Mennucci B, Amovilli C, Tomasi J (1998) Chem Phys Lett 286:221–225
27. Cammi R, Mennucci B, Tomasi J (1998) J Am Chem Soc 120:8834–8847
28. Albert IDL, Marks TJ, Ratner MA (1997) J Am Chem Soc 119:3155
29. Sheng Y, Jiang Y (1998) J Chem Soc Faraday Trans 94:1829
30. Schimdt MW et al. (1993) J Comput Chem 14:1347
31. Korambath PP, Karna SP (2000) J Phys Chem A 104:4801
32. Bogaard MP, Orr B (1975) J Phys Chem, series 2. In: Buckingham AD (ed) International review of science, vol 2. Butterworths, London p 149
33. Geskin VM, Lambert C, Bredas J-L (2003) J Am Chem Soc 125:15651–15658
34. Chandra AK, Uchimaru T (2001) J Phys Chem A 105:3578
35. Mandal K, Kar T, Nandi PK, Bhattacharyya SP, (2003) Chem Phys Lett 376:116–124
36. Nandi PK, Mandal K, Kar T (2003) Chem Phys Lett 381:230–238
37. Bartkowiak W, Misiaszek T (2000) Chem Phys 261:353 – 357

Contribution to Prof. Jug's 65th Birthday